ELR-CXC chemokine antagonism and cisplatin co-treatment additively reduce H22 hepatoma tumor progression and ameliorate cisplatin-induced nephrotoxicity

JING WEI[1*], XIANGYU CHEN[1*], QIANG LI[2], JIFEI CHEN[1], NOMAN KHAN[1], BING WANG[1], JYA-WEI CHENG[3], JOHN R. GORDON[4] and FANG LI[1]

[1]Department of Immunology, Dalian Medical University, Dalian 116044; [2]Jilin Medical College, Jilin 132013, P.R. China; [3]Institute of Biotechnology, Department of Life Science, National Tsing Hua University, Hsinchu 300, Taiwan, R.O.C.; [4]Division of Respirology, Critical Care and Sleep Medicine, Royal University Hospital, University of Saskatchewan, Saskatoon, SK S7N 0W8, Canada

Received October 3, 2013; Accepted December 16, 2013

DOI: 10.3892/or.2014.2996

Abstract. Cisplatin (*cis*-diamminedichloroplatinum) is one of the most commonly used agents for the chemotherapy of various types of cancers, but its use is limited by its dose-dependent side-effects (e.g., nephrotoxicity). The ELR-CXC chemokines are potent tumor growth, metastatic and angiogenic factors and can foster tumor resistance to chemotherapeutic agents. They are also potent proinflammatory agents. The aim of the present study was to evaluate the added effects of combining cisplatin chemotherapy with ELR-CXC chemokine antagonism in a mouse H22 hepatoma cancer cell model. The mice were injected with tumor cells and were then treated with cisplatin (12.5 or 2 mg/kg doses), either alone or together with the chemokine antagonist $CXCL8_{(3-72)}$ K11R/G31P (G31P) (50 μg/kg). At varying time-points renal function was examined using blood urea nitrogen (BUN) and serum creatinine (SCr) as read-outs for the toxic effects of cisplatin, while tumor growth and metastasis were assessed as endpoints. High-dose cisplatin therapy reduced the tumor burden by 52%, while co-delivery of G31P further augmented the tumor growth-suppressive effects of this dose of cisplatin to 71%; G31P by itself and low-dose cisplatin reduced the tumor burden by 19 and 39%, respectively. G31P also reduced the nephrotoxic effects of high-dose cisplatin to the effects observed in the low-dose cisplatin-treated animals. These data confirm the beneficial effects of combined cisplatin chemotherapy and ELR-CXC chemokine anatagonism in the context of both tumor progression and adverse side-effects.

Correspondence to: Dr John R. Gordon, Division of Respirology, Critical Care and Sleep Medicine, Royal University Hospital, University of Saskatchewan, Saskatoon, Room 2D30.8 Health Sciences Building, 107 Wiggins Road, Saskatoon, SK S7N 0W8, Canada
E-mail: john.gordon@usask.ca

Dr Fang Li, Department of Immunology, Dalian Medical University, 9 West Section, Lvshun South Road, Dalian 116044, P.R. China
E-mail: lifang16@hotmail.com

[*]Contributed equally

Abbreviations: G31P, $CXCL8_{(3-72)}$K11R/G31P; BUN, blood urea nitrogen; SCr, serum creatinine; RC, renal coefficient; qRT-PCR, quantitative real-time PCR; IHC, immunohistochemical; DAB, diaminobenzidine; PBS, phosphate-buffered saline; VEGF, vascular endothelial growth factor; H&E staining, hematoxylin and eosin staining; KC, keratinocyte-derived chemokine; MIP2, macrophage inflammatory protein-2; DNA, deoxyribonucleic acid; ATR, ATM/Rad3-related; cFLIP, cellular FLIP; FLIP, FLICE (caspase-8) inhibitory protein

Key words: cisplatin, CXCR1/R2 antagonist, acute renal failure, H22 hepatoma cancer cells

Introduction

Cisplatin is widely used for the treatment of many types of malignancies, but it results in a number of toxic side-effects, the most serious of which is nephrotoxicity (1). Cisplatin has dose-dependent toxic and pro-apoptotic effects on kidney cells (2), and it is also associated with the local release of inflammatory cytokines/chemokines and consequent inflammatory cell infiltration (1,3-6). It has been hypothesized that this inflammatory infiltration into the damaged kidney tissues further aggravates the cisplatin-induced nephrotoxic effects. Importantly, however, it was found that neutrophil depletion had no impact on cisplatin-induced renal function or tubular necrosis in a mouse model, suggesting that neutrophil infiltration could be a downstream effect of cisplatin-induced injury rather than a central driver of this pathology (7).

The seven ELR-CXC chemokines together play important roles in the recruitment of neutrophils in inflammatory responses, and act through their specific receptors, CXCR1 and CXCR2 (8). $CXCL8_{(3-72)}$K11R/G31P (G31P), which has been generated as both bovine (9,10) and human (11,12) CXCL8 analogues, is a full-spectrum ELR-CXC chemokine antagonist that has high affinity for both CXCR1 and CXCR2 (9,12). It

blocks ELR-CXC chemokine signal transduction through both receptors, such that it has broad-spectrum anti-inflammatory activity (13-15). It has also been shown to desensitize a number of heterologous G protein-coupled receptors (e.g., the receptors for C5a or fMLP) on CXCR1- or CXCR2-expressing cells, suggesting that its anti-inflammatory effects could be multi-modal (12). Moreover, given the roles of the ELR-CXC chemokines as tumor growth and angiogenic factors (16), it makes sense that G31P also possessed potent inhibitory effects on the growth, metastasis and angiogenesis of malignant tumors in a mouse model of human prostate cancer; indeed, it had anti-neoplastic effects comparable to those of Taxol (17). The ELR-CXC chemokines also foster the development of resistance to the cytotoxic effects of chemotherapeutic agents (18,19), such that antagonizing their activities might be predicted to augment therapeutic outcomes with these agents. In the present study, we assessed the impact of G31P and cisplatin co-treatment on tumor progression and cisplatin-related renal failure in an H22 hepatoma cell model of cancer.

Materials and methods

Reagents. The following reagents were purchased: cisplatin (Jiangsu Hansoh Pharmaceutical Co., Ltd., Jiangsu, China); RNAiso Plus, RT reagent kit with gDNA Eraser, and SYBR Premix Ex Taq II (Takara Bio Inc., Dalian, China); anti-VEGF-D (Bioworld Technology, Inc); immunohistochemistry (IHC) kit (ZSGB-Bio., Beijing, China); and blood urea nitrogen (BUN) and serum creatinine (SCr) kits (Nanjing Jiancheng Bioengineering Institute, Nanjing, China).

Animal model and drug administration. All protocols followed the guidelines of ethics regarding the treatment of animals used in experiments. This project was approved by the Dalian Medical University Ethics Committee in China. Female C57BL/6J mice (6 weeks old; n=5-6 mice/group) were obtained from the Dalian Medical University Laboratory Animal Center and were randomly divided into 6 groups. Tumor-bearing mice were treated with saline, 2 mg/kg of cisplatin, 12.5 mg/kg cisplatin with or without 500 μg/kg G31P or 500 μg/kg G31P alone. A sixth group of healthy mice served as the normal control animals. We had previously optimized the dose of human G31P required for use in rodents (Gordon JR, unpublished data), as we had in multiple other species.

Tumor-bearing mice received $5x10^6$ H22 mouse hepatoma cells (0.2-ml volumes, s.c.). G31P treatment mice were administered G31P s.c. on alternative days, commencing 7 days after tumor implantation, while the remaining groups received normal saline in the same manner. Cisplatin treatment mice were administered either 12.5 mg/kg (high dose) or 2 mg/kg (low dose) cisplatin i.p., while the remaining mice received an equal volume of saline i.p. The clinical status and the body weight of each mouse were evaluated daily, and on day 21 all mice were sacrificed for assessment of tumor progression. The primary tumors were resected from each animal and weighed.

Monitoring of renal function. Blood samples were collected from the angular vein of the mice under pentobarbital sodium (50 μg/kg) at 4, 8, 12, 24, 48 and 72 h and at day 21 post-tumor cell implantation. Serum samples were stored at -20˚C for blood urea nitrogen (BUN) and serum creatinine (SCr) detection. BUN and SCr values were determined according to the supplier's instructions, as standard measures of renal function (2). In addition, the renal coefficient (RC) was determined for each animal as a surrogate measure of general kidney health (20). To do so, both kidneys were excised and weighed and the RC was calculated using the following formula: Kidney weight/body weight. The kidneys were then snap-frozen in liquid nitrogen, and stored at -80˚C prior to real-time PCR analysis.

Table I. Primer sequences and the length of amplification products.

Name	Primer sequences	Length of product (bp)
IL-1β	Forward: 5'-tgccacctttgacagtgatgag-3'	
	Reverse: 5'-tgatgtgctgctgcgagattt-3'	137
KC	Forward: 5'-gattcacctcaagaacatccaga-3'	
	Reverse: 5'-ggacacctttagcatctttgg-3'	160
MIP-2	Forward: 5'-aacatccagagcttgagtgtgac-3'	
	Reverse: 5'-gccttgcctttgttcagtatctt-3'	152
β-actin	Forward: 5'-agagggaaatcgtgcgtgac-3'	
	Reverse: 5'-caatagtgatgacctggccgt-3'	163

Real-time PCR analysis. RNA of renal tissues was isolated using RNAiso Plus kits according to the supplier's protocol. Total RNA was reverse transcribed into cDNA using Takara RT reagent kit with gDNA Eraser. Briefly, first the genomic DNA was eliminated from each sample by incubation at 42˚C for 5 min and then the reverse-transcription reactions were performed. PCR parameters were set as 37˚C for 15 min and 85˚C for 5 sec. The transcriptional levels of IL-1β, KC and MIP-2 were determined by quantitative real-time PCR (qRT-PCR) analysis with Takara SYBR Premix Ex Taq II. Melting curve analyses were used to verify the accuracy of the PCR products following the amplification reactions. The PCR-primer sequences are indicated in Table I. The PCR cycling parameters (40 cycles) were set as: pre-denaturation (95˚C for 30 sec); denaturation (95˚C for 5 sec); annealing (59˚C for 30 sec); and extension (72˚C for 1 min). The relative expression values were normalized to that of β-actin. The $2^{-\Delta\Delta CT}$ method was used for analysis of the data.

Immunohistochemical detection of VEGF-D. Mice were sacrificed after 21 days of treatment and each tumor was resected and weighed. Solid tumor samples were fixed in 4% paraformaldehyde and embedded in paraffin using standard procedures in preparation for immunohistochemical (IHC) detection of VEGF-D. Briefly, endogenous peroxidase was blocked with 3% H_2O_2 for 10 min at room temperature. Afterward, the samples were rinsed three times with PBS (5 min each), incubated for 20 min at room temperature with normal goat serum as a blocking agent, washed as above with PBS and then incubated overnight at 4˚C with the primary

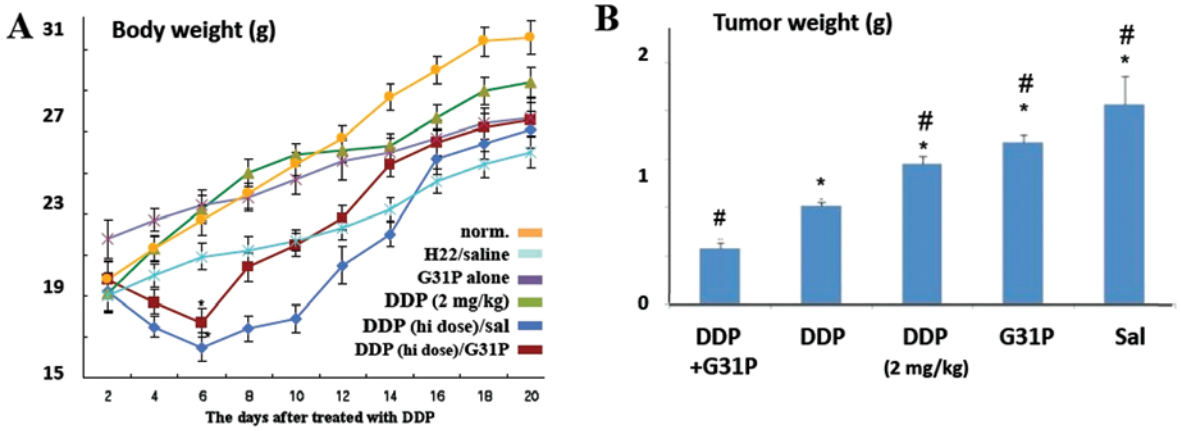

Figure 1. Impact of cisplatin chemotherapy and co-treatment with the ELR-CXC chemokine antagonist G31P on body weight and primary tumor weight in a mouse model of H22 hepatoma cell cancer. C57BL/6 (B6) mice were injected with 5x10^6 H22 mouse hepatoma cells s.c., and were then treated with saline (H22/sal), low-dose cisplatin [DPP (2 mg/kg)], high-dose cisplatin either alone [DPP (hi dose)/sal] or with 500 μg/kg of the ELR-CXC chemokine antagonist CXCL8$_{(3\text{-}72)}$K11R/G31P [DPP (hi dose)/G31P] or with G31P alone. We also included a normal healthy control group (norm.). (A) At the indicated times, we determined the body weight of each animal. (B) On day 21 after tumor injection we euthanized the mice and determined the weight of their primary tumors. $^{\#}$P≤0.05 vs. high-dose cisplatin alone; *P≤0.05 vs. G31P + high-dose cisplatin. DDP, cisplatin.

antibody (1:100 dilution). The tissues were again washed with PBS (3 times for 2 min each), incubated for 1 h at 37˚C with the secondary antibody, washed again with PBS as above, incubated in diaminobenzidine (DAB) solution for 10 min and counterstained with hematoxylin. The staining results were assessed by image analysis using the Microsoft Image-Pro 6.0.

Statistical analysis. Statistical analysis of the data and inter-group comparisons were carried out using the Student's t-test (two-tailed). Probability values of <0.05 were considered to indicate statistically significant results. The results are expressed as means ± SEM.

Results

Combined treatment with an ELR-CXC chemokine antagonist and cisplatin augments the tumor growth-suppressive effects of chemotherapy. Upon examination, we found that, overall, the tumor-bearing mice gained less weight than the healthy normal control mice (Fig. 1A). All cisplatin-treated animals displayed reduced activity, hypotrichosis, lackluster attitude and anorexia during the first 72 h following drug treatment. The 12.5 mg/kg dose cisplatin treatment led to substantial loss of body mass during the first 6 days post-treatment, whether or not the animals were co-treated with G31P, while the mice treated with G31P only or a 2 mg/kg dose of cisplatin lost no weight during this period. Weight gain in the high-dose cisplatin-treated tumor-bearing animals remained suppressed for the first 2 weeks, while G31P co-treatment ameliorated this effect somewhat. On day 21, all tumor-bearing mice weighed significantly less than the healthy control mice (P≤0.05; Fig. 1A).

On day 21 we also assessed the weight of the primary tumor in each animal and found that G31P treatment alone reduced the sizes of the primary tumors by 19%, while treatment with 2 mg/kg cisplatin reduced the tumor mass by 29%. High-dose cisplatin treatment alone reduced the size of the tumors in our mice by 52% (Fig. 1B; P≤0.05), and the addition of G31P co-therapy to this cisplatin treatment further enhanced the growth-suppressive effect observed, such that these tumors were 71% smaller than those in the saline-treated tumor-bearing mice (P≤0.05; Fig. 1B). The effect of high-dose cisplatin and G31P co-treatment on the progression of the primary tumors was additive.

Combined treatment of G31P and cisplatin reduces lymph node tumor metastasis. As VEGF-D expression is strongly linked to tumor dissemination via metastasis (21,22), we assessed expression of VEGF-D in our H22 hepatoma cell tumors using immunohistochemical methods and image analysis (Fig. 2). We observed strong expression of VEGF-D in the tumors of the saline-treated mice, and neither treatment with the ELR-CXC chemokine antagonist G31P alone nor low-dose cisplatin therapy had discernible effects on this expression. In contrast, high-dose cisplatin therapy, either alone or in combination with G31P co-therapy, reduced expression of VEGF-D in the tumors by ~50% (Fig 2B). Given the associations between VEGF-D production and metastatic disease, and the prognostic implications of extrahepatic metastasis in hepatocellular carcinoma (23), we also assessed the impact of ELR-CXC chemokine antagonism and cisplatin therapy on lymph node metastasis in our model. We resected the inguinal lymph nodes of our mice at the time of sacrifice and examined them directly for evidence of metastases using H&E-stained tissue sections (Fig. 3). We found abundant metastases in the lymph nodes of the saline-treated H22 hepatoma cell tumor-bearing mice, and evidence of metastases in the G31P only and low-dose cisplatin-treated animals. Few tumors were noted in the mice treated with high-dose cisplatin and particularly with the combination of G31P/high-dose cisplatin (Fig. 3).

Impact of CXCR1/CXCR2 antagonism on renal function in the cisplatin-treated hepatoma cell tumor-bearing mice. High-dose cisplatin therapy has been reported to induce renal inflammation and toxicity (2). Therefore, we assessed the expression of inflammatory mediators in our cisplatin and

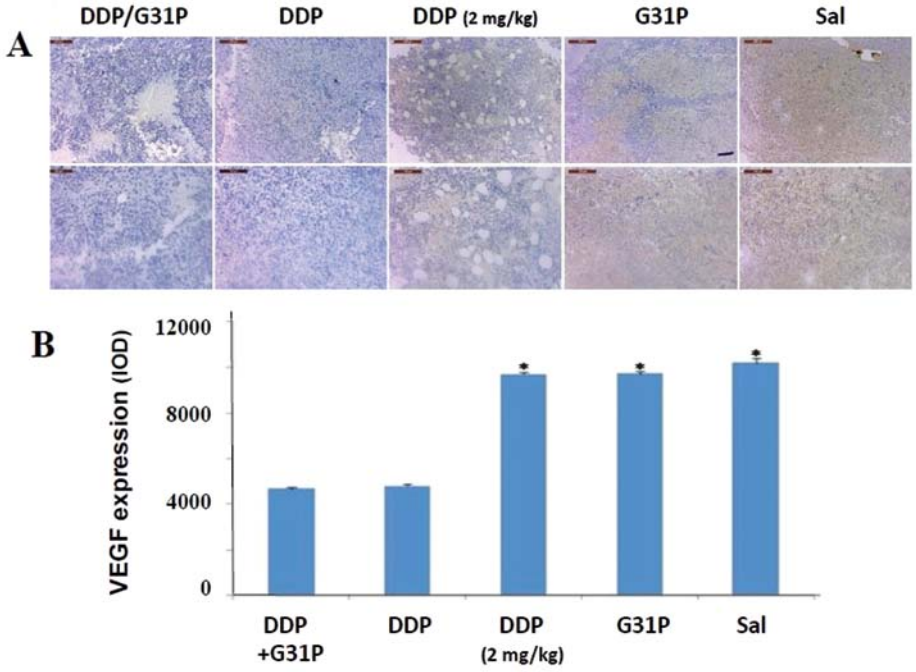

Figure 2. Impact of cisplatin and G31P co-treatment on intratumoral expression of metastasis-associated marker VEGF-D. H22 hepatoma tumors were established in B6 mice, and the animals were treated as described in Fig. 1 legend. At the time of tumor removal, paraffin sections of the tumor tissues were stained for immunohistochemistry for assessment of VEGF-D expression, which was quantified by image analysis, as described in Materials and methods. (A) Photomicrographs of representative VEGF-D-stained tissue sections. (B) Graphic representation of the results of the image analysis from the VEGF-D-stained tissue sections, presented as the mean (± SEM) integrated optical density (IOD). Sal, saline; DDP, cisplatin.

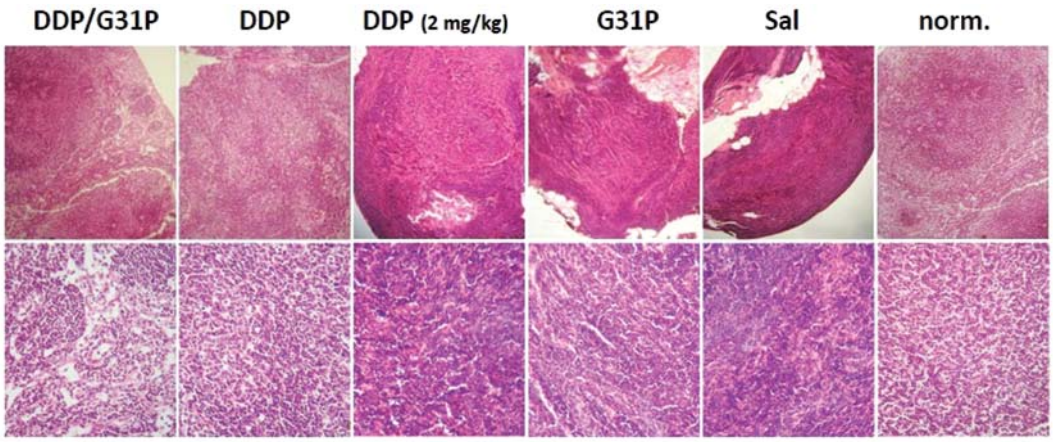

Figure 3. Impact of cisplatin and G31P co-treatment on inguinal lymph node metastasis in H22 hepatoma cell tumor-bearing mice. The inguinal lymph nodes of H22 hepatoma tumor-bearing mice treated as described in Fig. 1 legend were processed for histopathology and stained with H&E and then examined for evidence of hepatoma tumor metastases. The lymph nodes of the mice treated with saline (Sal), G31P and low-dose cisplatin (DDP 2 mg/kg) contained significant numbers of H22 hepatoma metastases, while the lymph nodes of the mice treated with high-dose cisplatin (DDP) and G31P/high-dose cisplatin (DDP/G31P) contained few metastases.

G31P-treated mice (Fig. 4), as well as the renal function, as determined by serum levels of blood urea nitrogen (BUN) and serum creatinine (SCr) and the renal coefficients (Fig. 5). We found that the saline- and G31P-treated mice displayed slight renal IL-1, KC and MIP2 expression thoughout the 3 days of observation (Fig. 4). Notably, the high- and low-dose cisplatin-treated mice expressed substantial levels of IL-1 during the 48 h following drug infusion, and the G31P co-treatment only modestly reduced this response. By day 3 the IL-1 response in the mice treated with low-dose cisplatin and G31P/high-dose cisplatin was again at background, while there remained a small IL-1 response at this time in the high-dose cisplatin-treated animals (Fig. 4A). The low-dose cisplatin treatment had a slight effect on inducing an ELR-CXC chemokine (i.e., KC or MIP2) response, while the high-dose cisplatin therapy markedly elevated the expression of both chemokines, albeit with distinct kinetics (Fig. 4B and C). The G31P co-treatment appeared to fully off-set the 8-h KC and MIP2 response to cisplatin, but by 48 h these animals also expressed substantial levels of both of these potent neutrophil agonists.

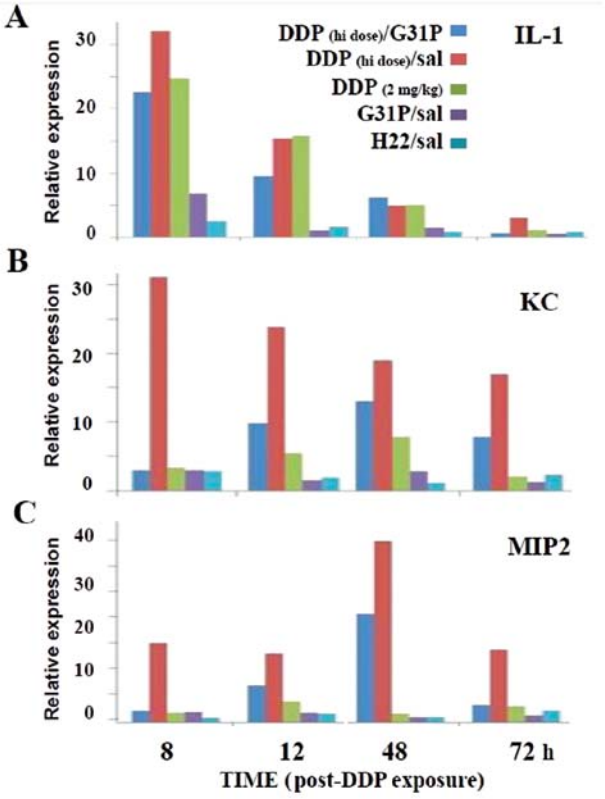

Figure 4. Impact of cisplatin and G31P co-treatment on renal expression of IL-1 and the ELR-CXC chemokines KC and MIP2. H22 hepatoma tumors were established in B6 mice, and the animals were treated as described in Fig. 1 legend. At the time of euthanasia, the expression of (A) IL-1, (B) KC and (C) MIP2 in the mouse kidneys was assessed by qRT-PCR, as described in Materials and methods. High-dose cisplatin therapy [DDP (hi dose)/sal)] strongly induced the expression of both ELR-CXC chemokines in the kidney tissues, while both high- and low-dose cisplatin [DDP (2 mg/kg)] induced IL-1 expression. G31P treatment significantly reduced, but did not eliminate, expression of any of these inflammatory mediators.

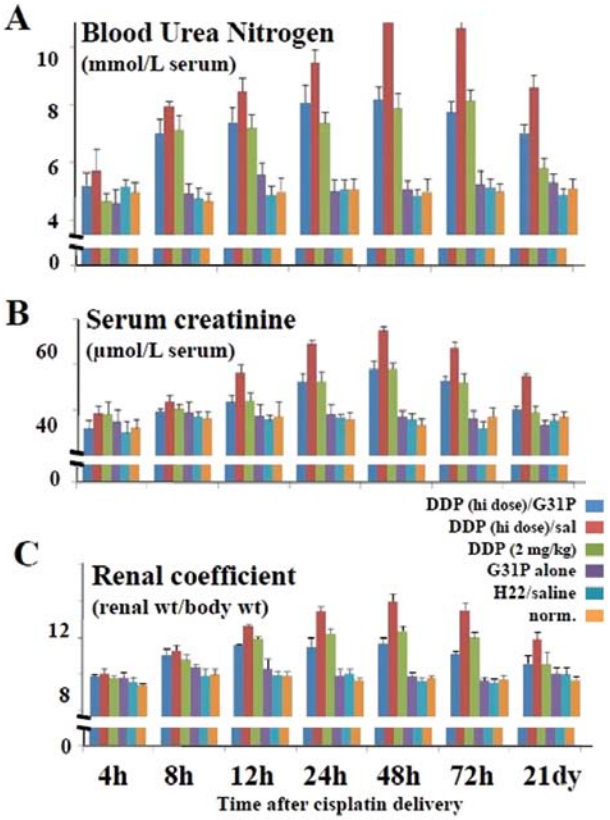

Figure 5. Impact of G31P co-treatment on cisplatin-induced nephrotoxicity in H22 hepatoma cell tumor-bearing mice. H22 hepatoma tumors were established in B6 mice, and the animals were treated as described in Fig. 1 legend. At the indicated times, serum was collected from the mice and assessed for (A) blood urea nitrogen (BUN) and (B) serum creatinine (SCr) as standard measures of renal toxicity. (C) The kidneys were excised and weighed, and the data were used to calculate the renal coefficient for each animal. The cisplatin therapies induced discernible dose-dependent nephrotoxicity, and the G31P co-treatment reduced the high-dose cisplatin-induced nephrotoxicity to the levels observed in the low-dose cisplatin-treated mice.

We also ascertained whether the mice were suffering from cisplatin-induced nephrotoxicity and whether CXCR1/CXCR2 antagonism had an impact. Neither the saline- nor the G31P only-treated hepatoma tumor-bearing mice displayed discernible evidence of kidney damage, while administration of cisplatin led to dose-dependent nephrotoxicity, as determined by increases in BUN, SCr and RC values (Fig. 5), with the high-dose therapy being overtly toxic. While G31P co-treatment significantly augmented the therapeutic outcome of high-dose cisplatin in terms of reducing tumor progression in our model, this combined therapy had a substantial beneficial impact on nephrotoxicity, as measured by serum levels of BUN and SCr and the RC values ($P \leq 0.05$, for G31P/high-dose cisplatin vs. high-dose cisplatin therapy alone). Indeed, the BUN and SCr levels in the mice treated with G31P/12.5 mg/kg cisplatin were approximately equivalent to those in the low-dose cisplatin-treated mice. Moreover, the RC values in the mice treated with G31P/high-dose cisplatin were lower overall than these values in the mice treated with low-dose cisplatin, indicating that co-delivery of G31P allowed the use of higher, more tumor-growth suppressive doses of cisplatin while at the same time protecting the animals against these cisplatin-associated toxic side-effects.

Discussion

We demonstrated that high-dose cisplatin chemotherapy was highly beneficial in terms of blocking H22 hepatoma tumor progression and metastasis, although this dose also caused substantial nephrotoxicity. More importantly, we also found that co-treatment with the CXCR1/CXCR2 antagonist G31P increased the antitumor activity of cisplatin, which was not unexpected given its reported antitumor activity in a mouse model of prostate cancer (17).

Cisplatin is a chemotherapeutic drug used clinically for the treatment of many types of cancers. In target cells it causes the formation of DNA adducts that activate multiple signal transduction pathways (e.g., ATR, p53, p73) that lead to tumor cell apoptosis (24). Yet, as it is excreted mainly by the kidneys, cisplatin causes substantial dose-dependent toxic renal side-effects even within its therapeutic dose (2). However, this toxicity is a compromise due to the therapeutic antitumor effects of the agent, yet this limits its use as a chemotherapeutic agent. Numerous chemotherapeutic agents induce the expression by tumor cells of ELR-CXC chemokines (e.g., CXCL8), which can reduce tumor cell death through regulation of the pro-apoptotic protein caspase-8-inhibitory protein c-FLIP

(reviewed in ref. 18). Indeed, we previously reported that G31P reverses the anti-apoptotic effects of the ELR-CXC chemokines on neutrophils (12). Thus, ELR-CXC chemokine antagonism might be expected to halt primary tumor progression, as noted above, and to reduce the toxicity of chemotherapeutic agents, thereby allowing the use of higher doses of these drugs with, consequently, better therapeutic outcomes. Our data confirmed that high-dose cisplatin therapy strongly induced intratumoral expression of the ELR-CXC chemokines KC and MIP2, while antagonizing these chemokines via G31P co-treatment reduced the nephotoxicity associated with high-dose cisplatin therapy to levels equivalent to those observed with low-dose cisplatin. While G31P should reduce some of the inflammatory responses observed in damaged kidneys, our data confirmed that it does not ablate this response, as assessed by expression of IL-1, KC or MIP2. This is consistent with the above-mentioned assumptions that neutrophil inflammation is not the primary cause of nephrotoxicity under cisplatin chemotherapy, but is rather a consequence of the toxicity (7). We hypothesized that G31P treatment activated anti-apoptotic processes in the kidneys of our cisplatin-treated mice and this was the mechanism behind its ability to reduce nephrotoxicity. Taken together, our results showed that ELR-CXC chemokine antagonism with an agent such as G31P can alleviate the renal injury caused by cisplatin without compromising its therapeutic efficacy. This approach may be clinically beneficial for the treatment of patients at risk for serious drug-induced renal injury.

Acknowledgements

The present study was supported by grants from the National Science Foundation of China (NSFC30772023) and the Natural Sciences and Engineering Research Council (NSERC) of Canada (J.R.G.).

References

1. Zernecke A, Weber KSC, Erwig LP, Kluth DC, Schroppel B, Rees AJ and Weber C: Combinatorial model of chemokine involvement in glomerular monocyte recruitment: role of CXC chemokine receptor 2 in infiltration during nephrotoxic nephritis. J Immunol 166: 5755-5562, 2001.
2. Miller RP, Tadagavadi RK, Ramesh G and Reeves WB: Mechanisms of cisplatin nephrotoxicity. Toxins 2: 2490-2518, 2010.
3. Eliopoulos N, Zhao J, Bouchentouf M, Forner K, Birman E, Yuan S, Boivin MN and Martineau D: Human marrow-derived mesenchymal stromal cells decrease cisplatin renotoxicity in vitro and in vivo and enhance survival of mice post-intraperitoneal injection. Am J Physiol Renal Physiol 299: F1288-F1298, 2010.
4. Fram RJ: Cisplatin and platinum analogues: recent advances. Curr Opin Oncol 4: 1073-1079, 1992.
5. Gonçalves GM, Zamboni DS and Câmara NO: The role of innate immunity in septic acute kidney injuries. Shock 34 (Suppl 1): 22-26, 2010.
6. Matsushima H, Yonemura K, Ohishi K and Hishida A: The role of oxygen free radicals in cisplatin-induced acute renal failure in rats. J Lab Clin Med 131: 518-526, 1998.
7. Faubel S, Lewis EC, Reznikov L, Ljubanovic D, Hoke TS, Somerset H, Oh DJ, Lu L, Klein CL, Dinarello CA and Edelstein CL: Cisplatin-induced acute renal failure is associated with an increase in the cytokines interleukin (IL)-1β, IL-18, IL-6, and neutrophil infiltration in the kidney. J Pharmacol Exp Ther 322: 8-15, 2007.
8. Mukaida N: Pathophysiological roles of interleukin-8/CXCL8 in pulmonary diseases. Am J Physiol Lung Cell Mol Physiol 284: L566-L577, 2003.
9. Li F, Zhang X and Gordon JR: $CXCL8_{(3-73)}$K11R/G31P antagonizes ligand binding to the neutrophil CXCR1 and CXCR2 receptors and cellular responses to CXCL8/IL-8. Biochem Biophys Res Commun 293: 939-944, 2002.
10. Li F, Zhang X, Mizzi C and Gordon JR: $CXCL8_{(3-73)}$K11R/G31P antagonizes the neutrophil chemoattractants present in pasteurellosis and mastitis lesions and abrogates neutrophil influx into intradermal endotoxin challenge sites in vivo. Vet Immunol Immunopathol 90: 65-77, 2002.
11. Zhao X, Li F, Town JR, Zhang X, Wang W and Gordon JR: Humanized forms of the CXCR1/CXCR2 antagonist, bovine $CXCL8_{(3-74)}$K11R/G31P, effectively block ELR-CXC chemokine activity and airway endotoxemia pathology. Int Immunopharmacol 7: 1723-1731, 2007.
12. Zhao X, Town JR, Li F, Zhang X, Cockcroft DW and Gordon JR: ELR-CXC chemokine receptor antagonism targets inflammatory responses at multiple levels. J Immunol 182: 3213-3222, 2009.
13. Gordon JR, Li F, Zhang X, Wang W, Zhao X and Nayyar A: The combined CXCR1/CXCR2 antagonist $CXCL8_{(3-74)}$K11R/G31P blocks neutrophil infiltration, pyrexia, and pulmonary vascular pathology in endotoxemic animals. J Leukoc Biol 78: 1265-1272, 2005.
14. Zhao X, Town JR, Li F, Li W, Zhang X and Gordon JR: Blockade of neutrophil responses in aspiration pneumonia via ELR-CXC chemokine antagonism does not predispose to airway bacterial outgrowth. Pulm Pharmacol Ther 23: 22-28, 2010.
15. Zhao X, Town JR, Yang A, Zhang X, Paur N, Sawicki G and Gordon JR: A novel ELR-CXC chemokine antagonist reduces intestinal ischemia reperfusion-induced mortality, and local and remote organ injury. J Surg Res 162: 264-273, 2010.
16. Waugh DJ and Wilson C: The interleukin-8 pathway in cancer. Clin Cancer Res 14: 6735-6741, 2008.
17. Liu X, Peng J, Sun W, Yang S, Deng G, Li F, Cheng JW and Gordon JR: G31P, an antagonist against CXC chemokine receptors 1 and 2, inhibits growth of human prostate cancer cells in nude mice. Tohoku J Exp Med 228: 147-156, 2012.
18. Wilson C, Purcell C, Seaton A, Oladipo O, Maxwell PJ, O'Sullivan JM, Wilson RH, Johnston PG and Waugh DJ: Chemotherapy-induced CXC-chemokine/CXC-chemokine receptor signaling in metastatic prostate cancer cells confers resistance to oxaliplatin through potentiation of nuclear factor-kappaB transcription and evasion of apoptosis. J Pharmacol Exp Ther 327: 746-759, 2008.
19. Wilson C, Wilson T, Johnston PG, Longley DB and Waugh DJ: Interleukin-8 signaling attenuates TRAIL- and chemotherapy-induced apoptosis through transcriptional regulation of c-FLIP in prostate cancer cells. Mol Cancer Ther 7: 2649-2661, 2008.
20. Kim YS, Moon JI, Kim DK, Kim SI and Park K: Ratio of donor kidney weight to recipient bodyweight as an index of graft function. Lancet 357: 1180-1181, 2001.
21. Jüttner S Wissmann C, Jons T, Vieth M, Hertel J, Gretschel S, Schlag PM, Kemmner W and Hocker M: Vascular endothelial growth factor-D and its receptor VEGFR-3: two novel independent prognostic markers in gastric adenocarcinoma. J Clin Oncol 24: 228-240, 2006.
22. Moldobaeva A, Baek A, Eldridge L and Wagner EM: Differential activity of pro-angiogenic CXC chemokines. Microvasc Res 80: 18-22, 2010.
23. Katyal S, Oliver JH III, Peterson MS, Ferris JV, Carr BS and Baron RL: Extrahepatic metastases of hepatocellular carcinoma. Radiology 216: 698-703, 2000.
24. Siddik and Zahid H: Cisplatin: mode of cytotoxic action and molecular basis of resistance. Oncogene 22: 7265-7279, 2003.